

Zirconia-Related Phases in the Zirconia/Titanium Diffusion Couple After Annealing at 1100°–1550°C

Kun-Lin Lin and Chien-Cheng Lin^{*,†}

Department of Materials Science and Engineering, National Chaio Tung University, Hsinchu 30050, Taiwan

A diffusion couple of 3 mol% Y_2O_3 - ZrO_2 and titanium was isothermally annealed in argon at temperatures between 1100° and 1550°C. The phases and microstructure in the ceramic side were investigated using scanning electron microscopy and transmission electron microscopy, both attached to an energy-dispersive spectrometer. After annealing at 1100°C/6 h, zirconia grains did not grow conspicuously and evolved only traces of oxygen, resulting in t - ZrO_{2-x} but not α -Zr. At temperatures above 1300°C, a significant amount of oxygen evolved from zirconia, reducing the O/Zr ratio, such that α -Zr was excluded from t - ZrO_{2-x} during cooling, yielding a higher O/Zr ratio (≈ 2). When held at 1550°C/6 h, zirconia grains grew rapidly. The α -Zr was segregated on grain boundaries during cooling by the exsolution of zirconium from ZrO_{2-x} , while twinned t' - ZrO_{2-x} or lenticular t - ZrO_{2-x} , which was embedded in ordered c - ZrO_{2-x} , was found. The ordered c - ZrO_{2-x} was identified by the $\frac{1}{5}$ {113} superlattice reflections of its electron diffraction patterns.

I. Introduction

EXTENSIVE research^{1–3} has been performed on the reactions between titanium and zirconia (ZrO_2), mostly using microhardness measurements, metallographic, and X-ray diffraction analyses. Economos and Kingery¹ indicated that titanium penetrated along the grain boundaries of ZrO_2 , without the formation of a new phase, other than the black oxygen-deficient zirconia (ZrO_{2-x}). Weber *et al.*² discovered limited dissolution of titanium in zirconia, as well as the blackening of zirconia, when the melting titanium reacted with the ZrO_2 crucible. Ruh³ found that up to 4 at.% of titanium was retained at room temperature as a substitutional solid solution in zirconia, while up to approximately 10 mol% zirconia would be dissolved in titanium, with zirconium and oxygen entering into the substitutional and interstitial positions of titanium lattice, respectively.

The darkening of yttria-stabilized zirconia was observed at high temperatures under reducing conditions.^{4,5} Moya *et al.*^{6,7} attributed the darkening of partially stabilized zirconia to the formation of Zr^{3+} ions. Using the electron spin resonance method, they claimed that the difference in color could be caused by the exsolution of impurities, mainly iron, from the bulk to the surface of zirconia polycrystals under reducing conditions. In contrast, other studies found^{8,9} black-colored zirconia following the formation of nonstoichiometric ZrO_{2-x} , where x indicates the deviation from stoichiometry. Rice¹⁰ stated that the zirconia was blackened by loss of intrinsic oxygen. Ingo¹¹ indicated that the change of valence states of zirconium was responsible for darkening of 8 wt% yttria-zirconia plasma-sprayed thermal barrier

coatings, while the segregation and exsolution of impurities (Fe, Al, Si, and Na) could be ruled out as causes of darkening.

The phase transformations of zirconia have been subjected to comprehensive investigations in the past several decades.^{12–20} In a systematic study on 12 wt% Y_2O_3 - ZrO_2 , Chaim *et al.*²¹ showed that a tweed-like microstructure existed inside c - ZrO_2 , resulting from the strain field of small coherent t - ZrO_2 precipitates after sintering at 1600°C/2 h. While a twinned t' - ZrO_2 phase with antiphase domain boundaries was observed after a subsequent annealing at 1550°C/1 h and a rapid cooling, twinned t - ZrO_2 precipitates (or colonies) among the c - ZrO_2 matrix were found after long-term annealing at 1400°C. However, precipitate-free zones at the perimeter of c - ZrO_2 grains with fine t - ZrO_2 precipitates were observed after annealing at 1250°C. The twinned t' - ZrO_2 phases, which resulted from the untransformable t - ZrO_2 , were characterized by a high Y_2O_3 content up to 10 wt% as mentioned in several other previous studies.¹⁷ The twins were able to relieve the strains arising from the small tetragonality of the product phase and the small molar volume change accompanying transformation.

Previous studies^{1–3} mentioned above did not deal with the fine features and new phases (except α -Zr) formed in the reaction zone of zirconia and titanium because of the instrumental limitation. Using analytical transmission electron microscopy (TEM), Lin and Lin²² characterized the microstructure abutting the interface of Ti melt and ZrO_2 . They reported that the liquid–solid reaction at 1750°C/7 min caused zirconia to transform into oxygen-deficient zirconia (ZrO_{2-x}) with an O/Zr ratio as low as 1.53. While a significant amount of oxygen accumulated at grain boundaries of titanium, the remainder was dissolved in titanium as α -Ti(O). An ordered titanium suboxide (Ti_3O) was then formed from a solid solution of α -Ti(O) during cooling. Moreover, the twinned α -Zr(O) was excluded from ZrO_{2-x} , leading to the formation of fine crystalline ZrO_{2-x} with a high O/Zr ratio (≈ 1.9) during cooling. The lamellae of Ti_2ZrO and α -Ti(Zr, O) were also found by TEM/energy-dispersive spectrometer (EDS) analysis.

In the heat-treatment experiments of the ZrO_2 /Ti diffusion couple conducted recently by Lin and Lin,²³ the lamellar and the spherical Ti_2ZrO as well as the orthorhombic β' -Ti were found to exist in the titanium side after annealing at 1550°C/30 min. On heating, the dissolution of a large amount of zirconium and oxygen into titanium gave rise to the metastably supersaturated disordered α -Ti(Zr, O) solid solution where Ti_2ZrO subsequently precipitated, while the β -Ti coexisting with α -Ti at high temperatures was transformed to the orthorhombic β' -Ti during cooling. However, the microstructural variation of zirconia in the reaction-affected zone has not been studied thoroughly to date. The purpose of the present study is to investigate the phases and microstructure of zirconia in the Ti/ ZrO_2 diffusion couple annealed at 1100°C to 1550°C for 6 h using scanning electron microscopy (SEM) and TEM, both attached to an EDS.

II. Experimental Procedures

Bulk ZrO_2 specimens used in this study were prepared from the powder of 3 mol% Y_2O_3 partially stabilized zirconia (>94 wt%)

D. Green—contributing editor

Manuscript No. 20333. Received March 22, 2005; approved May 8, 2005.

The authors would like to thank the National Science Council of Taiwan for financially supporting this research under Contract No. NSC 91-2216-E-009-021.

^{*}Member, American Ceramic Society.

[†]Author to whom correspondence should be addressed. e-mail: chienlin@faculty.nctu.edu.tw

ZrO₂+HfO₂, 5.4 wt% Y₂O₃, <0.001 wt% Fe₂O₃, <0.01 wt% SiO₂, <0.005 wt% Na₂O, <0.005 wt% TiO₂, <0.02 wt% Cl, <0.005 wt% SO₄²⁻; Toyo Soda Mfg. Co., Tokyo, Japan) by hot pressing (Model HP50-MTG-7010, Thermal Techno. Inc., Santa Rosa, CA). The specimens were heated to and held at 300°C for 3 min under 5 MPa at a heating rate of 30°C/min, while heating to and being held at 1450°C for 30 min under 30 MPa at a heating rate of 25°C/min. During cooling, pressure was released at 1100°C, and then the furnace was cooled down to room temperature.

The as hot-pressed ZrO₂ and commercially available pure titanium (with a nominal composition of 99.31 wt% Ti, 0.25 wt% O, 0.01 wt% H, 0.03 wt% N, 0.10 wt% C, 0.30 wt% Fe, designated as Cp-Ti hereafter) were cut and machined to the dimensions of 14 mm × 14 mm × 5 mm. Their surfaces were ground and polished to 0.5 μm using a diamond paste, and were then ultrasonically cleaned in acetone. The Cp-Ti was inserted in between two ZrO₂ specimens to form a sandwiched sample, and then placed in a graphite furnace; it was pressed in a preparatory process at 5 MPa, before the furnace was evacuated to 2 × 10⁻⁴ Torr and then filled with argon to a pressure of one atmosphere. This cycle of evacuation and purging was repeated at least three times. The temperature was increased to 1000°C at a rate of 30°C/min, and then to 1100°, 1300°, and 1550°C at 25°C/min, respectively, where the specimen was then held for 6 h. During cooling, the temperature was lowered to room temperature at a rate of 25°C/min and then the pressure was released.

The cross-sectional TEM specimens perpendicular to the interface of zirconia and titanium were cut into pieces of approximately 3 mm × 2 mm × 0.5 mm. They were ground down to ~80 μm thickness with a diamond matted disk, polished with diamond pastes of 6, 3, and 1 μm in sequence, dimpled to 50 μm thickness, and finally milled by precision ion milling (Model 691, Gatan Inc., Pleasanton, CA). The microstructure of the zirconia side in the reaction-affected zone was characterized using an SEM (Model JSM-6330F, JEOL Ltd., Tokyo, Japan) and an analytical TEM (Model JEM 2000FX, JEOL Ltd.) equipped with an EDS (Mode ISIS300, Oxford Instrument Inc., London, U.K.). The quantitative composition analyses were performed based on the principle of the Cliff-Lorimer²⁴ standardless method.

III. Results and Discussion

(1) Annealing at 1100°C

Figure 1(a) displays the TEM micrograph of the *t*-ZrO_{2-x} or tetragonal-deficient oxygen zirconia in the ceramic side of the

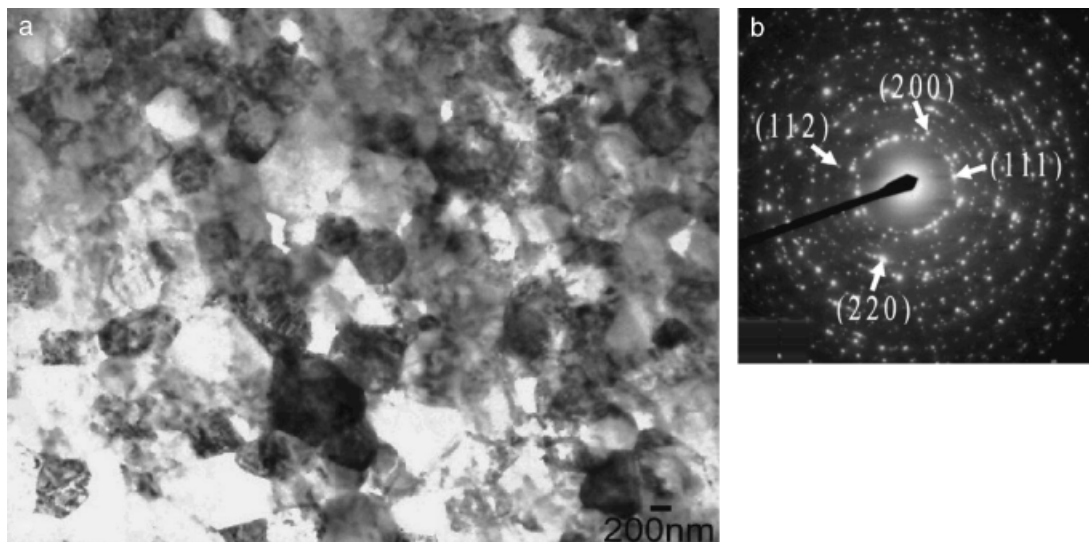


Fig. 1. (a) Transmission electron microscopy micrograph (bright field image) of zirconia far away from the ZrO₂/Ti interface after reaction at 1100°C/6 h, indicating *t*-ZrO_{2-x} with an average grain size of ~0.5 μm; (b) selected area diffraction pattern of the *t*-ZrO_{2-x}.

ZrO₂/Ti diffusion couple after reaction at 1100°C/6 h. An average *t*-ZrO_{2-x} particle size of around 0.5 μm is obtained so that no grain growth was noticeable. Figure 1(b) shows the diffraction ring pattern of the *t*-ZrO_{2-x}. The first, second, third, and fourth rings correspond to the *t*-ZrO_{2-x} {111}, {200}, {112}, and {220} planes, respectively. No phases other than the oxygen-deficient zirconia were found in the ceramic side.

(2) Annealing at 1300°C

Figure 2 displays an SEM micrograph (backscattered electron image (BEI)) of the zirconia side of the ZrO₂/Ti diffusion couple after reaction at 1300°C/6 h. The micrographs reveal the coexistence of α -Zr, labeled as "A" (bright), and *t*-ZrO_{2-x}, labeled as "B" (gray). The mean particle size of both α -Zr and *t*-ZrO_{2-x} was approximately 1 μm. The α -Zr appeared brighter than the ZrO_{2-x} in the BEI because of the atomic number effect. Also shown in Fig. 2, the dark areas represent voids, and a coarser intergranular α -Zr is shown by the arrow.

Figure 3 (a) displays the TEM micrograph of α -Zr and *t*-ZrO_{2-x}, corresponding to Fig. 2 on the zirconia side of the ZrO₂/Ti diffusion couple after reaction at 1300°C/6 h. The selected area diffraction pattern (SADP) of α -Zr, shown in Fig. 3(b), was identified as that of a hexagonal structure with $a \approx 3.18$ Å and $c \approx 5.01$ Å. Figure 3(c) shows the EDS spectrum of α -Zr, which reveals a composition of 81.03 at.% Zr, 15.29 at.% O, and 3.68 at.% Y. Figure 3(d) displays the SADP of *t*-ZrO_{2-x} on the zone axis of [110] with parameters $a \approx 5.05$ Å and $c \approx 5.14$ Å. Figure 3(e) presents the EDS spectrum of *t*-ZrO_{2-x}, consisting of 33.29 at.% Zr, 61.45 at.% O, and 5.26 at.% Y corresponding with ZrO_{1.846}. It is consistent with the fact that a two-phase region of α -Zr (O) and *t*-ZrO_{2-x} with a wide range of oxygen content (30.8 at.% O–63.5 at.% O) exists in the phase diagram of Zr–O at 1300°C. It also indicates that the solubility of α -Zr in tetragonal ZrO_{2-x} declined as the temperature decreased.²⁵ Hence, the α -Zr (O) tends to get segregated from the supersaturated solid solution of ZrO_{2-x} during cooling, and excluding Zr can increase the O/Zr ratio of the oxygen-deficient zirconia.

(3) Annealing at 1550°C

Figure 4(a) shows a BEI at the zirconia side of the ZrO₂/Ti diffusion couple after reaction at 1550°C/6 h. It reveals the coarsening of intergranular α -Zr (marked as "A") and *t*-ZrO_{2-x} (marked as "B") in the *c*-ZrO_{2-x} matrix (marked as "C"). The α -Zr was approximately 10 μm in size. Parts of the α -Zr easily peeled off to form voids (black) at the grain boundaries of zirconia by mechanical grinding and polishing. The grain size of the

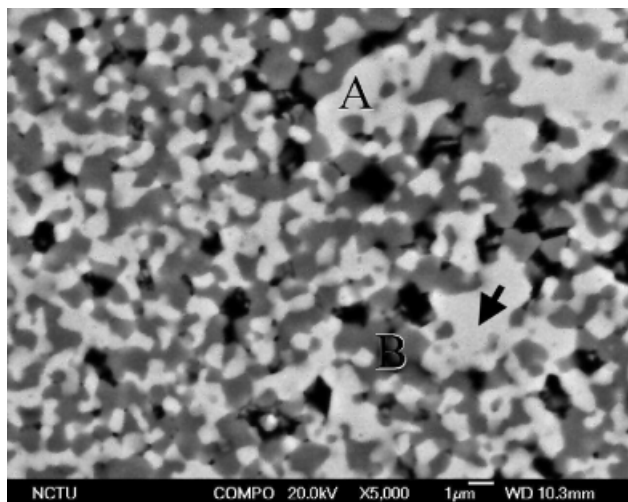
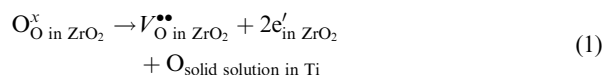


Fig. 2. Scanning electron microscopy micrograph (backscattered electron image) of the zirconia side in the ZrO_2/Ti diffusion couple after reaction at $1300^\circ C/6$ h, indicating the coexistence of α -Zr (marked as "A") and t - ZrO_{2-x} (marked as "B"). Also shown is the coarsening of α -Zr (arrowed).

zirconia matrix was about $50 \mu m$ on average, which was much larger than that of zirconia after reaction at either 1100° or $1300^\circ C$.

The high chemical affinity of titanium to oxygen, as well as the high solid solubility of oxygen in titanium (about 14.5%), is the driving force of the oxidation–reduction reaction, causing the formation of oxygen-deficient zirconia (ZrO_{2-x}) and α phase in titanium (oxygen-stabilized α phase). The oxidation–reduction reaction can be demonstrated by the following reaction:



The oxygen vacancies, resulting from the reduction reaction of ZrO_2 by Ti on annealing, as indicated by Eq. (1), were believed to dominate in the present study, even though the equilibrium concentration of oxygen vacancies increases with temperature. It is well known that vacancy is the predominant diffusion mechanism in zirconia, and the oxygen vacancies increase with the deviation from stoichiometry. Therefore, the atoms diffuse more rapidly with decreasing O/Zr ratio because of the reduction reaction of oxygen-deficient zirconia. The grain growth of ZrO_{2-x} during annealing at high temperatures is thus enhanced in that the grain growth is governed by the diffusion phenomenon.

The rate of oxidation–reduction reaction between zirconia and titanium increased with temperature, leading to a significant increase in oxygen vacancies or diffusivity, and an enhanced grain growth of ZrO_{2-x} as well. In contrast, the grain size of as hot-pressed zirconia, which was subjected to the same heat treatment as the zirconia/titanium diffusion couple, was about $2\text{--}3 \mu m$ on average as shown in Fig. 4(b). This fact indicates that the reaction between zirconia and titanium played a very important role in grain growth. During cooling, α -Zr was segregated on grain boundaries by the exsolution of zirconium from ZrO_{2-x} . The segregation of α -Zr in the grain boundaries can suppress further grain growth of ZrO_{2-x} because of the dragging effect. It is evidenced that no intragranular α -Zr was observed in the present study.

Figure 5(a) presents the TEM micrograph at the zirconia side of the ZrO_2/Ti diffusion couple after the reaction at $1550^\circ C/6$ h. The twinned t' - ZrO_{2-x} was embedded in the t' - ZrO_{2-x} matrix. Reflections of the type *odd, odd, even*, not allowed for c - ZrO_2 , were applied extensively to distinguish the c - ZrO_2 from the t - ZrO_2 phase. A $\langle 111 \rangle$ zone axis orientation was used as all possible t - ZrO_2 variants were identified using $\{112\}$ -type reflections.^{12–20} Figures 5(b) and (c) show the microdiffraction patterns of the t' - ZrO_{2-x} matrix and the twin t' - ZrO_{2-x} , respectively, with the electron beam along the zone axis $[111]$. The fact that reflections $\{112\}$ were absent in Figs. 5(b) and (c) indicated that both the matrix and the twin were tetragonal rather than cubic ZrO_{2-x} . These results were basically in agreement with the observations conducted by Heuer *et al.*^{16,17,21},

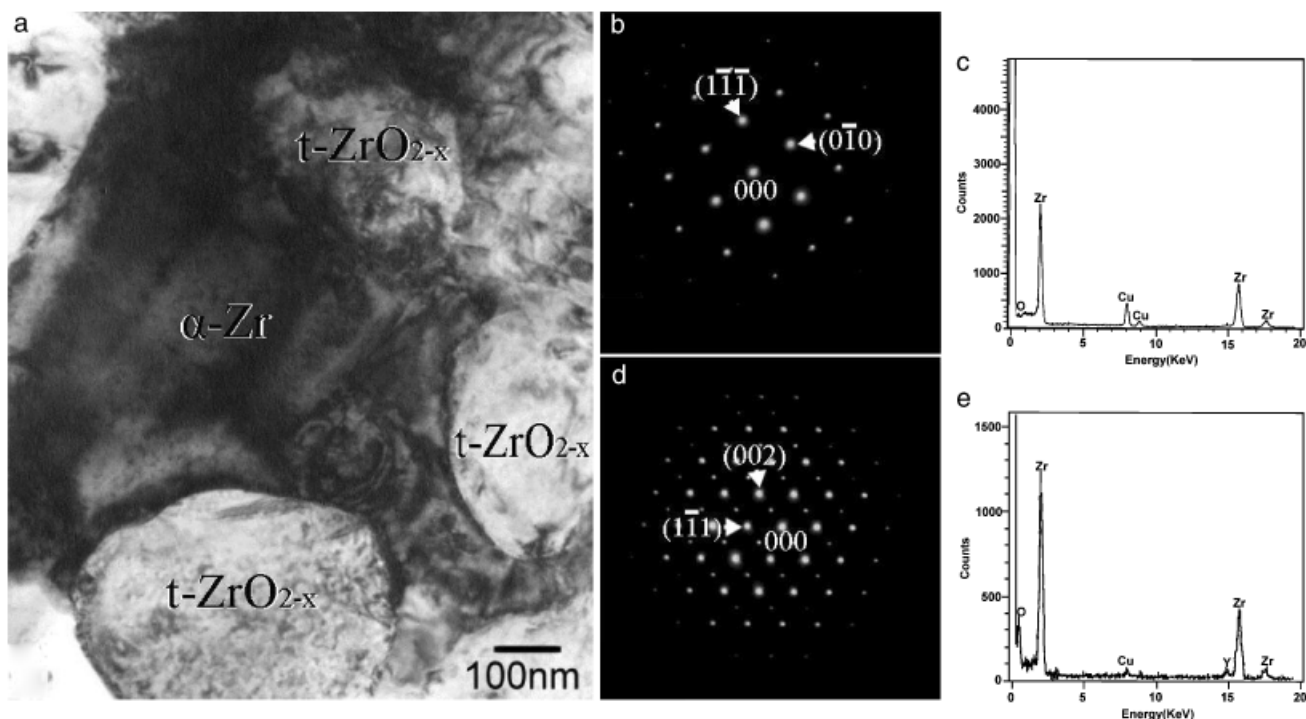


Fig. 3. (a) Transmission electron microscopy micrograph (bright field image) of α -Zr and t - ZrO_{2-x} in the ZrO_2/Ti diffusion couple after reaction at $1300^\circ C/6$ h; (b) selected area diffraction pattern (SADP) of the α -Zr along the $[101]$ zone axis; (c) an energy-dispersive spectrum of the α -Zr shown in (b); (d) SADP of the t - ZrO_{2-x} , along the $[110]$ zone axis; (e) an energy-dispersive spectrum of the t - ZrO_{2-x} shown in (d).

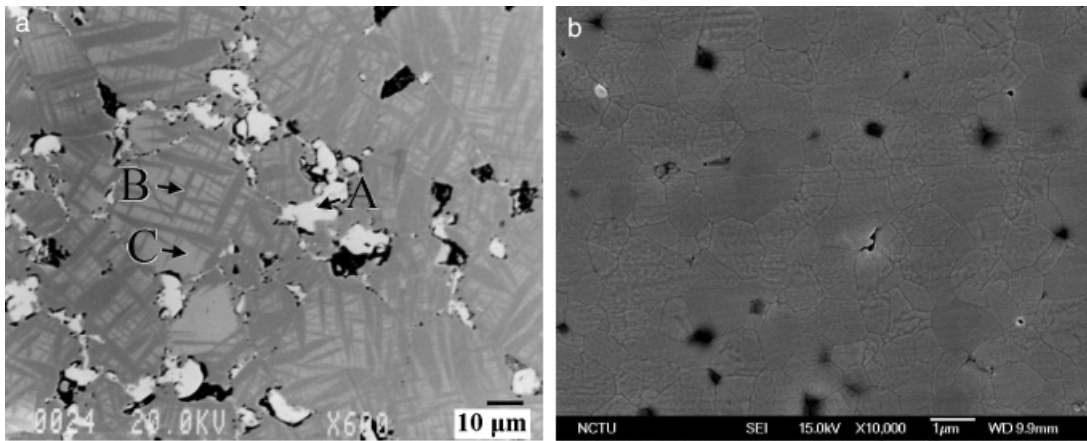


Fig. 4. (a) Scanning electron microscopy (SEM) micrograph (backscattered electron image) of the zirconia side in the ZrO_2/Ti diffusion couple after reaction at $1550^\circ C/6$ h, indicating the coarsening of intergranular α -Zr (marked as "A") and t - ZrO_{2-x} (marked as "B") in the c - ZrO_{2-x} matrix (marked as "C"); (b) SEM micrograph (secondary electron image) of as hot-pressed zirconia after annealing at $1550^\circ C/6$ h in Ar.

who described the displacive $c \rightarrow t'$ transformation in ZrO_2 alloys.

The ZrO_2 had a high Y_2O_3 content up to more than 10 wt% in previous studies;^{16,21} however, the Y_2O_3 concentration in ZrO_2 was as low as 5.36 wt% (3 mol%) in this study. According to the ZrO_2 - Y_2O_3 phase diagram, the ZrO_2 with 3 mol% Y_2O_3 at $1550^\circ C$ was predominantly tetragonal rather than cubic ZrO_2 ,²⁶ indicating that the $c \rightarrow t'$ displacive transformation could not have taken place in 3 mol% Y_2O_3 - ZrO_2 . However, a significant increase in oxygen vacancies, as a consequence of the reaction between zirconia and titanium, triggered the stabilization effect of zirconia. Therefore, it was inferred that the zir-

conia would be in the cubic phase solid solution region during annealing at $1550^\circ C$, and the t' phase was formed as the diffusion couple was cooled in a furnace to room temperature following annealing.

At a position further away from the interface, it was found that lenticular t - ZrO_{2-x} with three $\{100\}$ -type variants precipitated in the c - ZrO_{2-x} matrix on the zirconia side after annealing at $1550^\circ C/6$ h, as shown in Fig. 6(a). It was inferred that the specimen was cooled down from the two-phase ($c+t$) region in the ZrO_2 - Y_2O_3 phase diagram. On the other hand, the cubic oxygen-deficient zirconia would exist at $1550^\circ C$, as the eutectoid reaction, as expressed in the following equation, took place at about $1525^\circ C$:²⁷

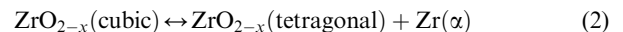


Figure 6(b) clearly shows, at a higher magnification, the contrast of the stress field because of the ordering of oxygen in the c - ZrO_{2-x} matrix. The EDS spectrum of c - ZrO_{2-x} , as shown in Fig. 6(c), revealed that lenticular t - ZrO_{2-x} consisted of 35.5 at.% Zr, 58.48 at.% O, and 6.02 at.% Y, corresponding to an oxygen-deficient zirconia of 7.25 mol% Y_2O_3 - $ZrO_{1.41}$. The lower limit of the solidus of the cubic ZrO_{2-x} phase lies in the range of $1.64 < O/Zr < 1.70$ between 1815° and $2065^\circ C$, while that for t - ZrO_{2-x} was 1.925 below $1300^\circ C$.^{27,28} It was not surprising that the measured O/Zr ratio in the present study was as low as 1.41 because of the intense oxidation-reduction reaction on annealing and sluggish diffusion during cooling. The SADPs of the c - ZrO_{2-x} matrix, with the zone axes being $[110]$ and $[310]$, are shown in Figs. 6(d) and (e), respectively. The fact that (112) reflections were absent in Fig. 6(d) confirmed that the matrix was c -symmetric in structure. The ordered structure was characterized by $\frac{1}{5}\{113\}$ superlattice reflections for zirconia unit cell in the mean time.

According to the Ellingham diagram, Ti cannot reduce the ZrO_2 . If the following reactions were applicable in the present study:



Then the oxidation-reduction reaction can be written as follows:



The Gibbs-free energy for the oxidation-reduction reaction (5) is $\Delta G = \Delta G_{\text{oxid}}(Ti) - \Delta G_{\text{oxid}}(Zr)$, where $\Delta G_{\text{oxid}}(Ti)$ and $\Delta G_{\text{oxid}}(Zr)$ are the Gibbs-free energies of oxidation of Ti and Zr, respectively. Based on the Ellingham diagram, the Gibbs-free energy

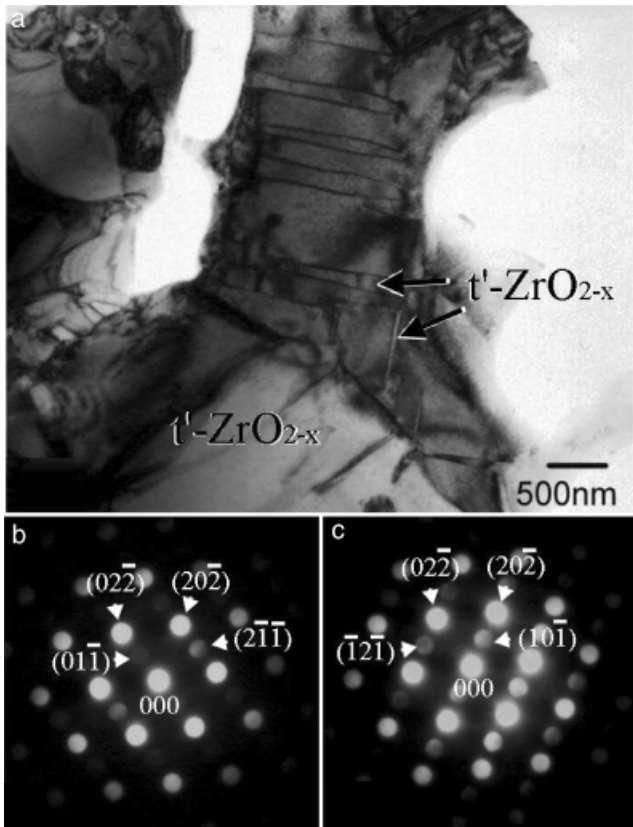


Fig. 5. (a) Transmission electron microscopy micrograph (bright field image) of zirconia in the ZrO_2/Ti diffusion couple after reaction at $1550^\circ C/6$ h, indicating the twinned t' - ZrO_{2-x} in t' - ZrO_{2-x} matrix; (b) and (c) show microdiffraction patterns from the twinned t' - ZrO_{2-x} and the t' - ZrO_{2-x} matrix along the zone axes of $[111]$, respectively.

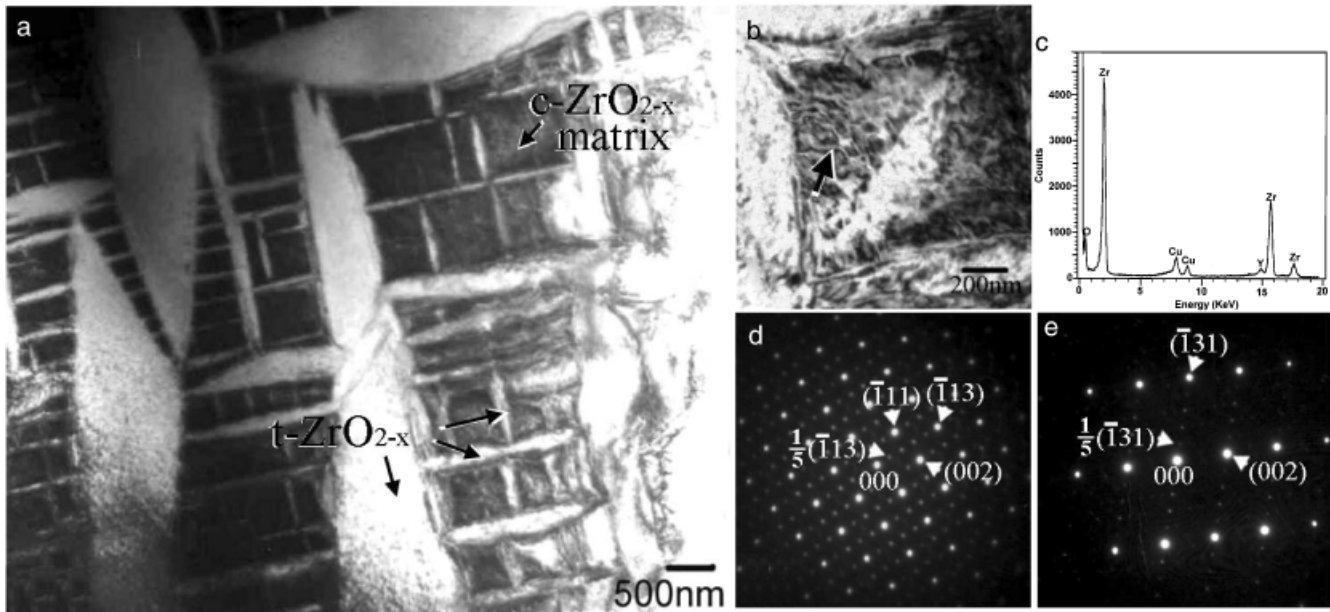
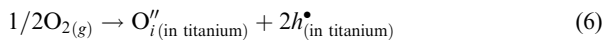


Fig. 6. (a) Transmission electron microscopy micrograph (bright field image) of zirconia in the ZrO_2/Ti diffusion couple after reaction at $1550^\circ C/6$ h, displaying $\{100\}$ -type variants of the lenticular $t-ZrO_{2-x}$ in $c-ZrO_{2-x}$ matrix; (b) a magnified image of the $c-ZrO_{2-x}$ matrix in (a), showing the ordered structure; (c) energy-dispersive spectrum of the ordered $c-ZrO_{2-x}$; (d) and (e) show selected area diffraction patterns of the ordered $c-ZrO_{2-x}$ matrix with the zone axes being $[110]$ and $[310]$, respectively.

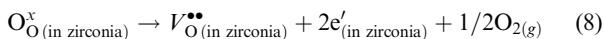
for the oxidation–reduction reaction (5) ΔG is positive, indicating that Ti cannot reduce ZrO_2 . However, this is not the case in the present study. Based on the experimental results, the following dissolution reaction should be applied:



The Gibbs-free energy of oxygen dissolution in solid titanium ΔG_{diss} is related to the temperature by the following equation:²⁹

$$\Delta G_{\text{diss}} = -RT \ln K_{\text{diss}} = -609 + 0.126T \quad (\text{kJ/mol}) \quad (7)$$

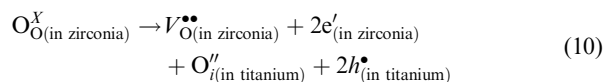
where K_{diss} is the equilibrium constant of reaction (6), R is the gas constant (≈ 8.3144 J/mol/K), and T is the absolute temperature. When $T = 1550^\circ C = 1823$ K, $\Delta G_{\text{diss}} = -379.30$ (kJ/mol). On the other hand, the reduction reaction of zirconia can be expressed as follows:



The Gibbs-free energy of the reduction reaction (8) ΔG_{red} can be calculated from the following equation:³⁰

$$\Delta G_{\text{red}} = -RT \ln K_{\text{red}} = -RT \left(2 - \frac{68\,000}{T} \right) \quad (9)$$

where K_{red} is the equilibrium constant of the reduction reaction (8), of which the nature logarithm is equal to $(2 - 68\,000/T)$. When $T = 1550^\circ C = 1823$ K, $\Delta G_{\text{red}} = 0.54$ (kJ/mol). The resultant reaction of reactions (6) and (8) is written using the following equation:



As $\Delta G = \Delta G_{\text{red}} + \Delta G_{\text{diss}} = 0.54 - 379.30 = -378.76$ (kJ/mol) at $1550^\circ C$, reaction (10) is thermodynamically favorable, consistent with the results observed in the present study.

(4) Proposed Model of Phase Development at $1300^\circ C$

The proposed model of microstructural evolution at the zirconia side of ZrO_2/Ti diffusion couple annealed at $1300^\circ C$ is schematically displayed in Fig. 7. In as hot-pressed zirconia, the grain size was about $0.3\text{--}0.4$ μm on average (Fig. 7(a)). On heating up to $1300^\circ C$, because titanium had a much higher affinity with oxygen than zirconium, ZrO_2 was dramatically reduced to

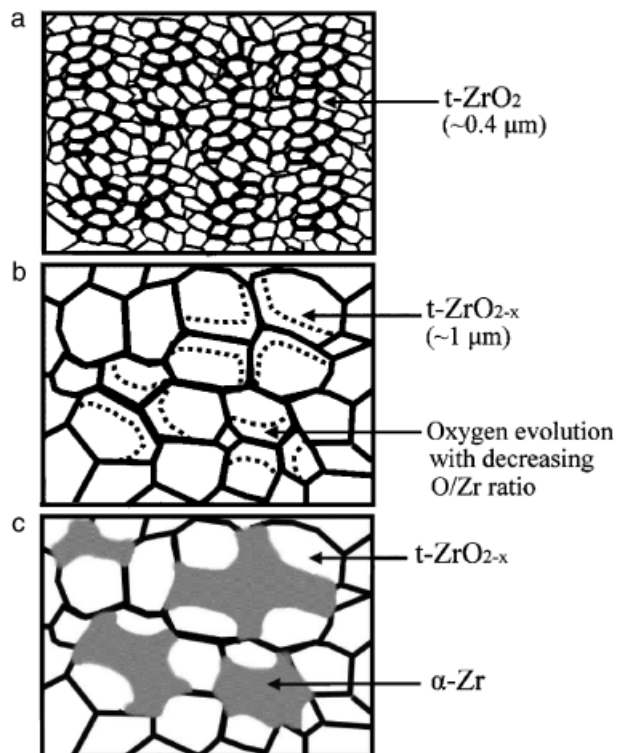


Fig. 7. Schematic diagrams showing the microstructural evolution of the zirconia side in the ZrO_2/Ti diffusion couple annealed at $1300^\circ C/6$ h. (a) As hot pressed; (b) grain growth on heating to $1300^\circ C$; (c) exclusion of $\alpha-Zr$ from ZrO_{2-x} during cooling.

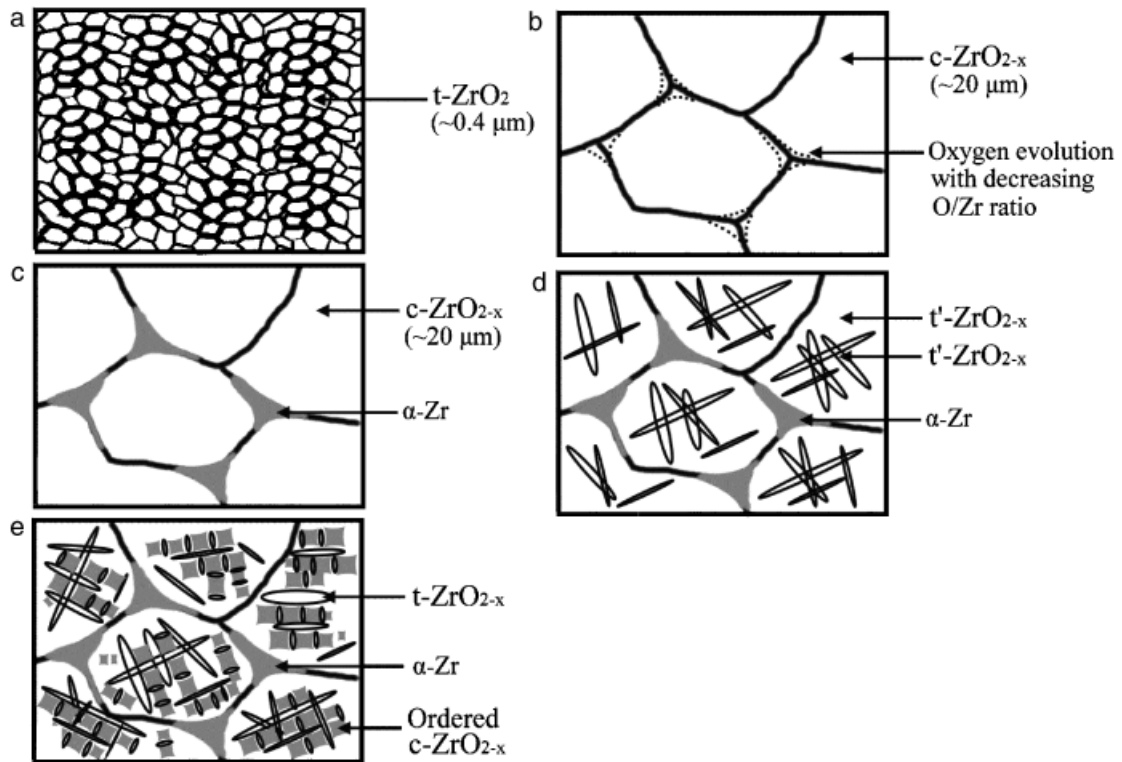


Fig. 8. Schematic diagrams showing the microstructural evolution of the zirconia side in ZrO_2/Ti diffusion couple annealed at $1550^\circ C/6$ h. (a) As hot pressed; (b) apparent grain growth on heating to $1550^\circ C$; (c) exclusion of $\alpha-Zr$ during cooling; (d) formation of twinned $t'-ZrO_{2-x}$; (e) the formation of lenticular $t-ZrO_2$ and ordered $c-ZrO_{2-x}$ during cooling.

ZrO_{2-x} by titanium and an insignificant grain growth occurred (Fig. 7(b)). During cooling, Zr was excluded from the unstable oxygen-deficient zirconia to the grain boundaries (Fig. 7(c)).

(5) Proposed Model of Phase Development at $1550^\circ C$

Figure 8 displays the schematic diagrams of microstructural evolution of the zirconia side in a hot-pressed ZrO_2/Ti diffusion couple annealed at $1550^\circ C$. In the heating stage, ZrO_{2-x} was initially formed following the intense oxidation–reduction reaction between zirconia and titanium as mentioned above. Then ZrO_{2-x} grains would grow rapidly because the vacancy diffusion was drastically enhanced (Fig. 8(b)). In the cooling stage, the $\alpha-Zr$ segregated on the grain boundaries of ZrO_{2-x} (Fig. 8(c)), causing the suppression of grain growth. The microstructure would be varied depending upon the distance from the interface. At the position close to the interface, the oxygen-deficient zirconia, with more concentrated oxygen vacancies, would be located in the single c -phase region and experience the displacive diffusionless $c \rightarrow t'$ transformation, resulting in twinned $t'-ZrO_{2-x}$ (Fig. 8(d)). At a position further away from the interface, it was believed that the oxygen-deficient zirconia, with less oxygen vacancies, was in the $(c+t)$ dual-phase region and the lenticular $t-ZrO_2$ with three variants precipitated in the ordered $c-ZrO_{2-x}$ (Fig. 8(e)).

IV. Conclusions

1. The diffusion couple of zirconia and titanium was isothermally annealed at temperatures ranging from 1100° to $1550^\circ C$. Three distinct microstructures were found depending upon the annealing temperature.

2. In the zirconia/titanium diffusion couple annealed at $1100^\circ C/6$ h, the $t-ZrO_2$ grain did not grow conspicuously and only a trace of oxygen evolved, yielding $t-ZrO_{2-x}$ without $\alpha-Zr$.

3. After annealing at $1300^\circ C/6$ h, more oxygen was evolved from zirconia, resulting in a decreasing O/Zr ratio. The $\alpha-Zr$ was excluded from $t-ZrO_{2-x}$, leading the O/Zr ratio to be close to 2.

4. When held at $1550^\circ C/6$ h, zirconia grains grew rapidly in addition to the intense oxidation–reduction reaction between zirconia and titanium. The $\alpha-Zr$ was segregated on grain boundaries during cooling by the exsolution of zirconium from ZrO_{2-x} , while twinned $t'-ZrO_{2-x}$ or lenticular $t-ZrO_{2-x}$, which was embedded in ordered $c-ZrO_{2-x}$, was found. The ordered $c-ZrO_{2-x}$ was identified by the $\frac{1}{5}\{113\}$ superlattice reflections of its electron diffraction patterns.

References

- G. Economos and W. D. Kingery, "Metal–Ceramic Interactions: II, Metal Oxide Interfacial Reactions at Elevated Temperatures," *J. Am. Ceram. Soc.*, **36** [12] 403–9 (1953).
- B. C. Weber, H. J. Garrett, F. A. Mauer, and M. A. Schwartz, "Observations on the Stabilization of Zirconia," *J. Am. Ceram. Soc.*, **39** [6] 197–07 (1956).
- R. Ruh, "Reaction of Zirconia and Titanium at Elevated Temperatures," *J. Am. Ceram. Soc.*, **46** [7] 301–6 (1963).
- W. S. Coblenz and R. W. Rice, "Methods of Oxidizing Reduced Ceramics"; U.S. Patent No. 4 568650, 1986.
- R. W. Rice, R. P. Ingel, B. A. Bender, J. R. Spann, and W. R. McDonough, "Development and Extension of Partially Stabilized Zirconia Single-Crystal Technology," *Ceram. Eng. Sci. Proc.*, **5** [7–8] 443–74 (1984).
- J. S. Moya, R. Moreno, J. Requena, and J. Soria, "Black Color Stabilized Zirconia," *J. Am. Ceram. Soc.*, **71** [11] C-479–80 (1988).
- J. Soria and J. S. Moya, "Reply to 'Comment on 'Black Color in Partially Stabilized Zirconia''," *J. Am. Ceram. Soc.*, **74** [7] 1747–8 (1991).
- J. H. Park and R. N. Blumental, "Thermodynamic Properties of Nonstoichiometric Ytria-Stabilized Zirconia at Low Oxygen Pressures," *J. Am. Ceram. Soc.*, **72** [8] 1485–7 (1989).
- P. Nicholson, "Influence of Reduction on Estimation of the ZrO_2 Tetragonal–Cubic Transformation Temperature," *J. Am. Ceram. Soc.*, **54** [1] 52–3 (1971).
- R. W. Rice, "Comment on Black Color in Partially Stabilized Zirconia," *J. Am. Ceram. Soc.*, **74** [7] 1745–6 (1991).
- G. M. Ingo, "Origin of Darkening in 8 wt% Ytria–Zirconia Plasma-Sprayed Thermal Barrier Coatings," *J. Am. Ceram. Soc.*, **74** [2] 381–6 (1991).
- M. Rühle, N. Claussen, and A. H. Heuer, "Microstructural Studies of Y_2O_3 -Containing Tetragonal ZrO_2 Polycrystals (Y-TZP)," pp. 352–70 in *Advances in Ceramics, Vol. 12, Science and Technology of Zirconia II*, Edited by N. Claussen, M. Rühle, and A. H. Heuer. American Ceramic Society, Columbus, OH, 1984.
- C. A. Andersson, J. Gregg Jr., and T. K. Gupta, "Diffusionless Transformations in Zirconia Alloys," pp. 78–85 in *Advances in Ceramics, Vol. 12, Science and Technology of Zirconia II*, Edited by N. Claussen, M. Rühle, and A. H. Heuer. American Ceramic Society, Columbus, OH, 1984.

- ¹⁴T. Sakuma, Y. I. Yoshizawa, and H. Suto, "The Microstructure and Mechanical Properties of Yttria-Stabilized Zirconia Prepared by Arc-Melting," *J. Mater. Sci.*, **20** [10] 2399–407 (1985).
- ¹⁵A. H. Heuer and M. Rühle, "Phase Transformations in ZrO₂-Containing Ceramic: I, The Instability of c-ZrO₂ and the Resulting Diffusion-Controlled Reactions"; pp. 1–13 in *Advances in Ceramics, Vol. 12, Science and Technology of Zirconia II*, Edited by N. Claussen, M. Rühle, and A. H. Heuer. American Ceramic Society, Columbus, OH, 1984.
- ¹⁶V. Lanteri, R. Chaim, and A. H. Heuer, "On the Microstructure Resulting from the Diffusionless Cubic→Tetragonal Transformation in ZrO₂-Y₂O₃ Alloys," *J. Am. Ceram. Soc.*, **69** [10] C-258–61 (1986).
- ¹⁷A. H. Heuer, "The Displacive Cubic→Tetragonal Transformation in ZrO₂ Alloys," *Acta Metall.*, **35** [3] 661–6 (1987).
- ¹⁸V. Lanteri, A. H. Heuer, and T. E. Mitchell, "Tetragonal Phase in the System ZrO₂-Y₂O₃"; pp. 118–30 in *Advances in Ceramics, Vol. 12, Science and Technology of Zirconia II*, Edited by N. Claussen, M. Rühle, and A. H. Heuer. American Ceramic Society, Columbus, OH, 1984.
- ¹⁹A. H. Heuer, V. Lanteri, and A. Dominguez-Rodriguez, "High-Temperature Precipitation Hardening of Y₂O₃ Partially-Stabilized ZrO₂ (Y-PSZ) Single Crystals," *Acta Metall.*, **37** [2] 559–67 (1989).
- ²⁰N. Ishizawa, A. Saiki, T. Yagi, N. Mizutani, and M. Kato, "Twin-Related Tetragonal Variants in Yttria Partially Stabilized Zirconia," *J. Am. Ceram. Soc.*, **69** [2] C-18–20 (1985).
- ²¹R. Chaim, M. Rühle, and A. H. Heuer, "Microstructural Evolution in a ZrO₂-12 wt% Y₂O₃ Ceramic," *J. Am. Ceram. Soc.*, **68** [8] 27–31 (1985).
- ²²K. F. Lin and C. C. Lin, "Transmission Electron Microscope Investigation of the Interface Between Titanium and Zirconia," *J. Am. Ceram. Soc.*, **82** [11] 3179–85 (1999).
- ²³K. L. Lin and C. C. Lin, "Ti₂ZrO Phases Formed in the Titanium and Zirconia Interface After Reaction at 1550°C," *J. Am. Ceram. Soc.*, **88** [5] 1268–72 (2005).
- ²⁴G. Cliff and G. W. Lorimer, "The Quantitative Analysis of Thin Specimens," *J. Microsc.*, **130** [3] 203–07 (1975).
- ²⁵H. Baker, *ASM Handbook, Vol. 3, Alloy Phase Diagrams*, p. 2326. ASM International, Metals Park, OH, 1992.
- ²⁶H. G. Scoot, "Phase Relationships in the Zirconia-Yttria System," *J. Mater. Sci.*, **10** [9] 1527–35 (1975).
- ²⁷R. J. Ackermann, S. P. Garg, and E. G. Rauh, "The Lower Phase Boundary of ZrO_{2-x}," *J. Am. Ceram. Soc.*, **61** [5–6] 275–6 (1978).
- ²⁸R. J. Ackermann, S. P. Garg, and E. G. Rauh, "High-Temperature Phase Diagram for the System Zr-O," *J. Am. Ceram. Soc.*, **60** [7–8] 341–5 (1977).
- ²⁹W. E. Wang and Y. S. Kim, "A Thermodynamic Evaluation of the Titanium-Oxygen System from O/Ti = 0 to 3/2," *J. Nucl. Mater.*, **270**, 242–7 (1999).
- ³⁰W. E. Wang and D. R. Olander, "Thermochemistry of the U-O and Zr-O Systems," *J. Am. Ceram. Soc.*, **76** [5] 1242–8 (1993). □